Tempo and mode of performance evolution across multiple independent origins of adhesive toe pads in lizards

Hagey, Travis J.; Uyeda, Josef C.; Crandell, Kristen E.; Cheney, Jorn A.; Autumn, Kellar; Harmon, Luke J.

Evolution

DOI:
10.1111/evo.13318

Published: 01/10/2017

Peer reviewed version

Tempo and Mode of Performance Evolution across Multiple Independent Origins of Adhesive Toe Pads in Lizards

Travis J. Hagey Corresponding Author, BEACON Center for Evolution in Action, Michigan State University, East Lansing, MI, USA, hageyt@egr.msu.edu
Josef C. Uyeda Department of Biological Sciences, University of Idaho, Moscow, ID, USA, josef.uyeda@gmail.com
Kristen E. Crandell Department of Zoology, University of Cambridge, CB2-3EJ, UK kec51@cam.ac.uk
Jorn A. Cheney Structure and Motion Laboratory, The Royal Veterinary College, University of London, Hatfield, UK, jcheney@rvc.ac.uk
Kellar Autumn Biology Department, Lewis & Clark College, Portland, OR, USA, autumn@lclark.edu
Luke J. Harmon Department of Biological Sciences, University of Idaho, Moscow, ID, USA, lukeh@uidaho.edu

Running Title Tempo and Mode of Adhesion Across Origins
Keywords Gecko, Anole, Toe Detachment Angle, Brownian Motion, Ornstein-Uhlenbeck

Word Count 6300
Table count 1
Figure Count 5
Data Accessibility Supplemental Material

Abstract

Understanding macroevolutionary dynamics of trait evolution is an important endeavor in evolutionary biology. Ecological opportunity can liberate a trait as it diversifies through trait space, while genetic and selective constraints can limit diversification. While many studies have examined the dynamics of morphological traits, morphological traits may have many-to-one mapping with respect to performance. As performance is often more proximately the target of selection, examining only morphology may give an incomplete understanding of evolutionary dynamics. Here we ask whether convergent evolution of pad-bearing lizards have followed similar evolutionary dynamics, or whether independent origins are accompanied by unique constraints and selective pressures over macroevolutionary time. We hypothesized that geckos and anoles each have unique evolutionary tempos and modes. Using performance data from 59 species, we modified Brownian Motion (BM) and Ornstein-Uhlenbeck (OU) models to account for repeated origins estimated using Bayesian ancestral state reconstructions. We discovered that adhesive performance in geckos evolved in a fashion consistent with Brownian Motion with a trend, whereas anoles evolved in bounded performance space consistent with more constrained evolution (an Ornstein-Uhlenbeck model). Our results suggest that convergent phenotypes can have quite distinctive evolutionary patterns, likely as a result of idiosyncratic constraints or ecological opportunities.

Introduction

When investigating how the diversity (or lack thereof) of a trait arose, one of the first steps is to observe the variation present in the trait and investigate how the trait evolved through time, asking whether the trait has thoroughly explored a small part of trait space, or if the trait appears to have freely explored trait space. Thorough coverage of a limited region of trait space can suggest constrained evolution, possibly due to limited developmental or genetic variation, biomechanical constraints, or limited ecological opportunity to adapt and change. Alternatively, a trait may appear to have explored trait space in a less constrained fashion. This may be due to fewer developmental, genetic, or biomechanical constraints, the trait accessing more open niches, or the trait being under weak selection, drifting through trait space with little consequence.

Knowledge of how a clade has evolved through trait space can be integrated into a fuller understanding of that clade's evolutionary history. For example, if a clade has exhibited constrained evolutionary patterns, future studies can investigate how the focal trait may be limited by developmental, genetic, or mechanical constraints, or how biotic interactions have influenced the diversification of the trait. For example, habitat use/morphology correlations have been reported to differ between Caribbean and South American anoles (Irschick et al. 1997; Macrini et al. 2003). These differences may suggest Caribbean and mainland anoles have filled trait space differently, possibly due to differences in development, genetics, biomechanical considerations, or differences in abiotic or biotic conditions in the Caribbean and mainland South America.

In addition to investigating the evolution of a morphological trait through trait space, if a focal trait is a measure of performance, as is the case in our study, knowledge of how restrictive its evolution has been through performance space can influence understanding of the underlying morphological evolution. Performance is often more closely related to the ecological function of a trait than is its morphology, which is only indirectly related to fitness; thus, the evolutionary dynamics of performance are of particular interest (Arnold 1983; Wainwright and Reilly 1994). Evidence suggesting a clade's performance has been constrained in performance space could be explained by a variety of situations. Focal clades may not have had the genetic, developmental, or mechanical capabilities to diversify and explore performance space, or there may have been limited niche space available to diversify into, similar to as if a focal trait was a morphological trait. In addition, when considering performance niche space, limited successful performance options do not impose limited underlying morphological diversity. Few adaptive options can lead to convergent or parallel morphological evolution, including many to one mapping, when different morphologies perform similarly. Alternately, evidence of unconstrained performance evolution could be explained by behavioral plasticity, phenotypic plasticity, adaptive change tracking adaptive peaks, as well as weak selection allowing for performance to drift through performance space.

Modeling the evolutionary history of a trait also requires some knowledge or assumptions about the origin or origins of the trait in question. While many studies have focused on the relationship between convergent morphology and performance, few studies have compared the tempo and mode of performance evolution in a comparative framework (but see Harmon et al.

2003). By focusing on convergent traits, we can better understand how limiting factors such as constraints or limited ecological opportunities have shaped the evolution of our focal clades.

Evaluating the fit of Ornstein-Uhlenbeck (OU) and Brownian motion (BM) models of trait evolution to a focal clade can identify how constrained (OU) or free (BM) the evolution of the trait has been (Lande 1976; Hansen 1997). Brownian motion models the diffusion of a trait through trait space with two parameters, the root value and a stochastic rate parameter (σ^2). Alternatively, OU models extend BM models to represent constrained evolution towards a target value (θ). OU has the additional parameter α, which describes the rate of pull towards the target trait value θ. As α gets smaller and approaches zero, an OU model converges towards a BM model. BM models can also be extended to model a directional trend when a third parameter, μ, is non-zero, modeling the tendency of the trait value to consistently drift in a particular direction (positively or negatively) away from the root value.

In this study, we examine the evolutionary dynamics of performance in two groups of squamates: geckos and anoles. Adhesive toe-pads have evolved at least three times in Squamata: most famously in geckos, but also twice outside of Gekkota, in anoles and skinks. We define adhesive toe pads as having morphological traits such as setae or modified scales that generate both friction and adhesion (frictional adhesion; Autumn et al. 2006a). The results from previous studies have suggested one (Harrington and Reeder 2017) or multiple origins of toe pads within the 1700 described species of geckos (Underwood 1954; Haacke 1976; Russell 1976; Russell 1979; Irschick et al. 1996; Russell 2002; Gamble et al. 2012; Russell et al. 2015; Higham et al. 2016; Gamble et al. 2017). The adhesive system of lizards is an excellent system for investigating patterns of adaptation, constraint, and convergence. Gecko and anole toe pads are morphologically complex, being comprised of modified ventral scales with a free edge (lamellae) covered in small hair-like structures called setae. There is considerable morphological diversity among species at the macroscale *i.e.*, toe pad shape, skeletal features, and digital musculature (Russell 1979; Gamble et al. 2012) and at the microscale *i.e.*, setal morphology (Ruibal and Ernst 1965; Williams and Peterson 1982; Peattie 2007; Johnson and Russell 2009; Hagey et al. 2014). These structures are responsible for the generation of adhesion and friction on a variety of surface textures, self-cleaning, and not self-adhering (Hansen and Autumn 2005; Vanhooydonck et al. 2005; Autumn et al. 2006a; Huber et al. 2007; Persson 2007; Russell and Johnson 2007; Pugno and Lepore 2008b; Hu et al. 2012; Autumn et al. 2014; Russell and

Johnson 2014) suggesting that while toe pads appear very diverse, there likely exists extensive constraints and limitations on their morphology and performance. It is likely that the evolution and adaptation of adhesive performance in padded lizards has balanced selective pressures and opportunities with mechanical and developmental constraints, likely limiting the options open to evolution and adaptation.

We considered how gecko and anole toe pad adhesive performance evolved by fitting a variety of stochastic models of trait evolution. We fit models with shared or independent parameter values and/or models across geckos and anoles, incorporating ancestral state reconstruction results into our models, to test the hypothesis that independent origins differ in rate (tempo) or pattern (mode). If a single-rate model is a good fit to our entire adhesive performance dataset, this would suggest that the performance of padded lizards and their convergent morphologies evolved under similar processes, shared mechanical, developmental constraints, and/or similar selection dynamics. In contrast, if clade-specific models or parameters fit our data well, this would reveal a pattern of clade-specific evolutionary dynamics, likely associated with clade-specific constraints or ecological opportunities (Hansen 1997; Butler and King 2004; Yoder et al. 2010; Eastman et al. 2013). Considering patterns of performance evolution in conjunction with ancestral information improves our understanding of how historical processes of adaptation have shaped extant diversity, morphology, and performance.

Methods.

Estimation of the number of origins of toe pads across Squamata

To identify independent origins of adhesive toe pads in lizards, we used a large, species-level phylogeny of Squamata (Pyron and Burbrink 2013). The use of this phylogeny requires some caveats. Large macrophylogenies, like the Pyron and Burbrink (2013) phylogeny may not be well suited for use in comparative method analyses (see Title and Rabosky 2016). This phylogeny also has topological differences as compared to other smaller published phylogenies (Sadlier et al. 2005; Brown et al. 2012; Gamble et al. 2012; Oliver et al. 2012). We chose a time-scaled, ultrametric tree because our models of trait evolution model trait change in relation to time rather than sequence divergence. We assigned presence or absence of toe pads to each species in the phylogeny (4162 species). Four species of skinks are known to have adhesive pads, *Prasinohaema virens, P. flavipes, P. prehensicauda, Lipinia leptosoma* (Williams and

Peterson 1982; Irschick et al. 1996; Pianka and Sweet 2005). Of the three pad-bearing *Prasinohaema* species, only *P. virens* is in the Pyron and Burbrink (2013) phylogeny. In addition, only one species of *Lipinia* is in the phylogeny (*L. pulchella*). We substituted *L. leptosoma* for *L. pulchella* without a loss of phylogenetic information (Austin 1998) for a total of two pad-bearing skink species in our toe pad presence/absence dataset. We assigned the presence of toe pads to all *Anolis* species in the phylogeny (207 species) except *A. onca* (Peterson and Williams 1981; Nicholson et al. 2006). To assign presence/absence to geckos, we modified generic-level assignments from Gamble et al. (2012) adding information from Wilson and Swan (2010) and personal observations (TH), to assign toe pad presence (472 species) or absence (188 species) to all 660 species of geckos in the phylogeny (see Fig. 3 and Supplemental Material). The remaining lizard and snake species in the tree were considered padless.

Using the complete phylogeny of Pyron and Burbrink (2013), we estimated the number of origins of adhesive toe pads across squamates by combining Bayesian estimates of transition rate matrices with stochastic character mapping. We estimated transition matrices for a binary-state, Mk model with asymmetric transition rates allowing the rates of pad gain and loss to vary (*i.e.,* q10 and q01 were not constrained to be equal) using the R package Diversitree (FitzJohn 2012). We then ran a Bayesian MCMC for 10,000 generations sampling every 100 generations, with an initial burn-in of 3,000 generations, resulting in a posterior sample of 701 Q matrices. To visualize our reconstructions, monomorphic clades were collapsed, resulting in a phylogeny with 118 tips. Using the posterior sample of Q-matrices, we generated 701 simmap phylogenies using the R function *make.simmap* in the phytools package (Revell 2012). Of particular interest was the number of independent origins of toe pads within geckos (Gamble et al. 2012). We therefore counted the number of estimated origins in Gekkota across the simmap-generated reconstructions to obtain a posterior sample of origins.

Collection of performance data

Previous studies of pad-bearing lizards have quantified adhesive performance in multiple ways (Irschick et al. 1996; Autumn et al. 2006a; Autumn et al. 2006b; Pugno and Lepore 2008a; Autumn et al. 2014; Hagey et al. 2014; Hagey et al. 2016). We chose to use the angle of toe detachment, which was first used to quantify adhesive performance in frogs (Emerson 1991; Moen et al. 2013) and subsequently in geckos (Autumn et al. 2006a; Hagey et al. 2014; Hagey et

al. 2016). The angle of toe detachment is directly related to the adhesive mechanics of setae (Autumn et al. 2006a; Tian et al. 2006) and can be measured easily in the laboratory or field with relatively simple equipment (see Supplemental Material). This approach quantifies the maximum proportion of adhesion (negative normal force), relative to friction, generated by a species' toe pad (see Fig. 1 and Methods). We quantified adhesive performance across three families of geckos (Gekkonidae, Phyllodactylidae, and Diplodactylidae) and the genus *Anolis* (see Supplemental Material). Our toe detachment observations were collected following previous studies, using captive and wild caught specimens from the field (Costa Rica, Panama, Thailand, and Australia) and the lab (Autumn et al. 2006a; Hagey et al. 2014; Hagey et al. 2016). We used a variety of equipment setups that included powered rotational stages, stepper motors (including Lego Mindstorm motors), and manual rotational stages. To measure angle of toe detachment, live non-sedated lizards were suspended via the toe pad of a single rear toe from a vertical glass microscope slide (Video links in Supplemental Material; Autumn et al. 2006a; Hagey et al. 2014; Hagey et al. 2016). Variation in performance across toes has not been previously investigated and so we strived to always test similar toes. Our trials alternated between the longest left and right rear toes, or the center rear toes if all rear toes were similar in length. Using a single toe eliminated confounding forces that would be generated by multiple toes acting in opposing directions. During each toe detachment trial, the glass substrate was initially vertical with the animal's toe pad generating friction relative to the substrate (and likely little adhesion *i.e.*, force perpendicular and towards the glass). The glass substrate was then slowly inverted. When this occured, the setal shaft angle increased, generating adhesion and friction relative to the glass. At the angle of toe detachment, the maximum ratio of adhesion to friction that the toe pad was capable of generating was exceeded, and the animal fell onto a cushioned pad (see Fig. 1 and video links in Supplemental Material). Toe-pad area has previously been shown to correlate with the amount of friction generated by anole toe pads (Irschick et al. 1996), presumably due to the fact that larger pads have more setae interacting with the substrate. This relationship has not been investigated regarding toe detachment angle. While we would not predict toe-pad area to correlate with toe detachment angle, due to the fact that detachment angle is weight independent and likely related to setal morphology (Autumn et al. 2006a) and not the absolute number of setae contacting the surface, this relationship still requires evaluation.

Our performance observations included measurements of over 250 individual lizards from 59 species (13 species of anoles and 46 species of geckos; Fig. 3; see Supplemental Material). Our dataset had a minimum of two observations per individual and maximum of 49, with a mean of 9.1 observations per individual. We collected five or more observations from 91% of the individuals sampled. Observations from each individual lizard were fit to a Weibull distribution, which is often used in "time-to-failure" analyses (McCool 2012). The Weibull scale parameter, with standard error, was then estimated, representing each individual's detachment angle (Hagey et al. 2016). To produce a mean value for each species, we calculated a weighted average using each individual's estimated Weibull scale value, weighting by the inverse of its estimated standard error. In six of our 59 focal species, we did not record individual identity for each performance trial; therefore we estimated performance of these species as if all observations were from a single individual (see Table S.1).

Modeling trait evolution

We performed all trait evolution analyses using untransformed performance data. Natural-log transforming our data would artificially emphasize differences between small detachment angles and reduce differences between large detachment angles. Our initial analyses fit single and multi-regime BM and OU models of trait evolution via a maximum likelihood approach with the use of *a priori* assigned clades using the R package OUwie (Beaulieu et al. 2012). We also conducted analyses not requiring *a priori* clade assignments using the R packages AUTEUR (Eastman et al. 2011), fitting multi-regime BM models, and SURFACE (Ingram and Mahler 2013), fitting multi-θ OU models (See Supplemental Material). In our OUwie analyses we considered seven models in total, including species mean errors. Our two simplest models were a Brownian motion model (BM1) and an Ornstein-Uhlenbeck model (OU1) that each fit a single set of parameters. Our other five models fit unique parameter values in various combinations to the gecko and anole clades. The decision to assign unique parameter values to anoles and geckos followed the results obtained from our ancestral state reconstruction, with anoles and geckos representing independent origins of toe pads, although we note that other studies have suggested multiple independent origins within geckos (see Introduction and Discussion). We fit the following models: a BM model with variable evolutionary rates (σ^2) and single root value (BMσ^2), an OU model with single α and σ^2 parameter value and different

optima (θ) values (OUθ), an OU model with a single α but multiple rate (σ^2) and optima (θ) parameter values (OUσ^2θ), an OU model with a single σ^2 but variable α and θ values (OUαθ), and a OU model (OUσ^2αθ) in which all three parameters, σ^2, α, and θ, varied (Table 1; Beaulieu et al. 2012). We then compared the fit of our seven models using AICc weights based on relative model likelihoods (Table 1; Burnham and Anderson 2002).

The models we have described so far can sometimes rely on unrealistic assumptions. These models estimate a trait value at the root, which is the phylogenetic weighted mean of tip states for our BM1 and OU1 models. In our case, toe pads have had multiple origins, with the backbone of the squamate phylogeny likely lacking toe pads. Our model assumptions regarding performance at the root of the tree, the most recent shared common ancestor of geckos and anoles, is inferred to have a performance that is near the average of geckos and anoles. This is almost surely in error. Incorrect root-node trait values can affect parameter estimate values and fit comparisons; for example, by allowing less change and/or a weaker α parameter value, mimicking Brownian Motion. To incorporate ancestral state information, we fit a set of BM and OU models that assumed independent origins for geckos and anoles using modified likelihood functions from the R packages *bayou* and *geiger* (Harmon et al. 2008; Pennell et al. 2014; Uyeda and Harmon 2014). We considered the lack of toe pads to have a performance value of 0°. Both the gecko and anole clades were assigned a root state of 0° and shifted to an OU or BM process model along their respective stem branch, with the timing of the initiation of the OU or BM model being allowed to vary along the branch, before diversification. When considering the likely evolution of setae from spinules, these simple early structures likely initially generated friction with little adhesion, which would result in a low detachment angle with higher detachment angles likely being achieved after the evolution of more complex setae (see Discussion). As a result, our assignment of detachment angles of 0° to padless species and the assumption that recently evolved toe pads have performance near zero is supported from a biomechanical and evolutionary point of view.

Stem branch dates were taken from the Pyron and Burbrink (2013) phylogeny. For geckos, the timing of the shift to an OU or BM process was constrained to occur between 168.8 mya (the timing of the divergence of geckos from other lizards) and 82.3 mya (the ancestral node of Gekkota). For anoles, the timing of the shift was constrained between 76.3 mya (the divergence of anoles from Corytophanidae) and 44.1 mya (the ancestral node of *Anolis*). We

again considered single and multi-regime models of BM and OU, constraining our OU models to a maximum θ value of 90° (no species has been observed sticking to a surface with one toe beyond an angle of 45°). A total of 9 models incorporating ancestral information were considered (models denoted by an asterisk, Table 1). We did not exhaustively fit all possible combinations of models, but instead let the results of earlier analyses guide our choices: BM with a shared σ^2 for both geckos and anoles (*BM1), Single-optimum OU with shared α and σ^2 parameters (*OU1), Brownian motion with a trend and shared mean, σ^2, and μ parameter, where μ describes the rate of the trend (*BMT), Brownian motion with a trend and shared σ^2, but different trend (μ) parameters for each clade (*BMTμ), an OU model with separate θ for each clade (*OUθ), OU with separate α and θ for each clade (*OUαθ), OU with separate σ^2 and θ for each clade (*OU $\sigma^2\theta$), OU with separate α, σ^2, and θ for each clade (*OU$\sigma^2\alpha\theta$), and lastly a BM model with a trend fit to geckos and an OU model fit to anoles (*BMT_G-OU_A). We computed AIC scores and AIC weights for each model using maximum likelihood optimization to evaluate which model was best supported by our data (Table 1). To supplement these analyses assuming one origin of toe pads within geckos, we also conducted a set of limited analyses assuming two origins of toe pads within Gekkota (see Supplemental Material).

In addition to this likelihood analysis, we fit the full *OU$\sigma^2\alpha\theta$ model using a Bayesian implementation in *bayou* (denoted *OU$\sigma^2\alpha\theta_{Bayesian}$ in Table 1). By considering our most complex model, we can compare posterior probabilities for inferring differences in parameters between clades. We set the following priors on the parameters: α ~ half-Cauchy(scale = 0.1), σ^2~ half-Cauchy(scale = 0.1), θ ~ Uniform(min = 0, max = 90). Shift locations were given uniform priors over the length of the stem branches for geckos and anoles. We ran four chains for 1,000,000 generations and discarded the first 30% of the samples as burn-in. We then combined all the chains and estimated the median and 95% highest posterior density (HPD) interval for each parameter value.

For use in our comparative modeling, we modified the Pyron and Burbrink (2013) phylogeny by removing unsampled taxa. In a few cases we replaced closely related unsampled taxa with taxa for which we had performance measurements. We replaced *Afroedura karroica* and one of the closely related *Geckolepis* species with *A. hawequensis* and *A. loveridgei*, possibly overestimating the divergence between our two sampled *Afroedura* species. We also

had performance observations from the recently described *Oedura bella*, substituting it for the closely related *O. gemmata* (Oliver et al. 2012; Oliver and Doughty 2016).

Results

Regarding our reconstruction of the number of independent origins of toe pads, our posterior sample of transition matrices had negligible autocorrelation for all parameters and high effective sample sizes, indicating convergence and adequate mixing. Transition rates were estimated to be highly asymmetric, with losses of toe pads occurring at rates an average of 16.8 times faster than gains (95% HPD 3.2 – 41.1). Our reconstruction favored three origins in squamates (geckos, anoles, and skinks, Fig. 2) but we were unable to rule out multiple origins within geckos. Within geckos, our reconstruction favored a single origin (53% of posterior reconstructions), followed by two origins (30%), with only 4% of reconstructions having three or more origins within geckos. 13% of our reconstructions contained no origins within geckos, modeling the root of squamates as having pads. It is worth noting that we observed some reconstructions in our posterior sample with transient assignments, in which toe pads transitioned from absent to present, back to absent along a single branch, generating no overall change but possibly inflating the number of origins we observed. In addition, we observed an origin of toe pads in the branch leading to *Hemidactylus* in 33% of our posterior reconstructions, complementing previous studies of toe pad origins in geckos (Fig. 2; Gamble et al. 2012).

We conducted a Shapiro-Wilk test of normality and found our performance data to not be significantly different from than expected for a normal distribution ($W = 0.98$, $p = 0.32$). We found toe detachment angle to vary widely across padded lizards (Fig. 3, Table S.1), ranging from 15° to over 40°. When we consider detachment angle among clades, we note detachment angle in anoles ranged from 15.7° to 23.3°; lower than in most gecko species. Gekkonid and phyllodactylid geckos showed the greatest variation, with detachment angles ranging from 23.4° to 40.5° (Fig. 3, Table S.1). Diplodactyline geckos exhibited intermediate performance between anoles and the gekkonids and phyllodactyls, exhibiting detachment angles between 15.0° and 30.1° (Fig. 3, Table S.1).

Considering our trait evolution analyses, our OUwie results did not find clear support for one particular model of trait evolution (Table 1). We found support for a single-rate BM model (BM1, AICc weight of 0.35) with weaker support for an OU model with clade specific σ^2, α, and

θ values, ($OU\sigma^2\alpha\theta$ model, AICc weight of 0.19). When we examine our $OU\sigma^2\alpha\theta$ model parameter estimates, geckos were modeled under an OU model with a very small α value ($2.1x10^{-9}$), large σ^2 (3.6), and distant θ (> 1000), which converges towards BM with a trend (Table 1). It is worth noting again that these models assume unrealistic ancestral states, with a phylogenetic mean performance value for the ancestor of geckos and anoles, which almost certainly did not have toe pads.

For our custom models of trait evolution, which improved upon our OUwie analyses by incorporating constrained root state and timing of parameter shifts, our best fitting model was one in which geckos evolved under a BM model with a trend, and anoles evolved under an OU model (*BMT_G-OU_A, AIC weight = 0.37; Fig. 4), followed closely by a global Brownian Motion with a trend model (*BMT, AIC weight = 0.35; Table 1). The third best-fitting model assigned unique μ values to geckos and anoles (*BMTμ, AIC weight = 0.18). When independent OU models are fit to geckos and anoles, the estimate for phylogenetic half-life in the gecko clade is 208.2 million years with an estimated θ of 90° (the maximum allowable performance value), compared to the short half-life estimated for anoles of 0.33 million years and a θ of 19.4°. Support for a BM model with a trend in geckos is indicative of very little statistical signal for bounded evolution, a surprising result given the bounded nature of performance space (detachment angle being constrained between 0° and 90°). This result is supported when assuming one or two origins in Gekkota (see Supplemental Material). By contrast, there is support for an OU model in anoles, in which anoles are very near their estimated θ value and have a very rapid phylogenetic half-life. However, possibly due to the limited sampling of *Anolis* species in our dataset (14 species), the *BMT and *BM_G-OU_A models are roughly equivalent when accounting for the fact that the *BMT model has only four parameters, while the *BM_G-OU_A model has seven.

Considering our *$OU\sigma^2\alpha\theta_{Bayesian}$ model, although we observed overlap among parameters estimated for geckos and anoles, the results again suggest that the phylogenetic half-life for anoles is shorter than that of the geckos, with anoles much closer to their θ value, whereas gecko evolution is relatively unconstrained (Fig. 5; Table 1). All parameter estimates reached stationarity and had effective sizes of over 200 and were similar to maximum likelihood estimates (Table 1).

Discussion

Our ancestral state reconstruction favored a single origin of toe pads within geckos, which is significantly fewer than previous work (Gamble et al. 2012), although we cannot rule out multiple origins (see Gamble et al. 2017). We also found toe detachment angle to be highly variable across species of padded lizards (14° to 40°, see Supplemental Material) and evidence supporting our hypothesis that independent toe pad origins would exhibit different tempos and modes of performance evolution. There was no evidence of substantial constraints on the evolution of gecko adhesive performance. In fact, we found consistent support for an unconstrained model of trait evolution in geckos, which indicates adhesive performance in geckos has evolved with ample evolutionary opportunity and few constrains. Conversely, anole performance appears to be limited to relatively low angles of toe detachment, suggesting strong constraints, consistent selection, or limited ecological opportunity.

Independent Origins of Toe Pads

Many previous studies have contributed to our understanding of independent toe pad origins within geckos (Underwood 1954; Haacke 1976; Russell 1976; Russell 1979; Irschick et al. 1996; Russell 2002; Higham et al. 2015; Russell et al. 2015; Higham et al. 2016), with recent studies suggesting between one (Harrington and Reeder 2017) and 11 origins (Gamble et al. 2012), including origins in the Phyllodactylidae family and on the stem of *Hemidactylus*. This is still a very active area of research (Gamble et al. 2017). Our reconstruction suggested a single origin at the base of geckos, although we did find some evidence suggesting *Hemidactylus* may represent an independent origin of toe pads within Gekkota (see Results, Fig. 2, and Supplemental Material), complementing results from Gamble et al. (2012), despite topological differences between the Gamble et al. (2012) and Pyron and Burbrink (2013) phylogenies regarding genera closely related to *Hemidactylus* (see Title and Rabosky 2016 regarding the use of macrophylogenies in comparative analsyes). In our analyses assumed the inferred rate of gains and losses applied across Squamata, Gamble et al. (2012) made a similar assumption while only considering geckos. This difference in scope may explain the discrepancy between our two studies. While neither our study nor the Gamble et al. (2012) study allowed the rate of pad gain or loss to vary across the tree, some clades may be predisposed to evolving or losing adhesive toe pads, resulting in clade-specific rates or gain or loss. There are multiple distantly related genera

of geckos that exhibit adhesive structures on the tips of their tails strikingly similar to those on their toes such as *Lygodactylus* in the Gekkonidae family and New Caledonia and New Zealand genera in the Diplodactylidae family (Bauer 1998). These independent origins of adhesive tail pads may suggest that geckos are predisposed to evolve adhesive pads, possessing easily co-optable developmental pathways as compared to other lizards.

In addition, if toe pad state is correlated with diversification rate, this may impact ancestral reconstruction results (Maddison 2006). Gamble et al. (2012) found toe pads to be associated with slightly higher rate of diversification, although this was not the case for Garcia-Porta and Ord (2013). Considering state-correlated diversification rate alongside an ancestral state reconstruction, Harrington and Reeder (2017) concluded a single origin of toe pads using a 'hidden states' binary-state speciation and extinction model (Maddison et al. 2007; Beaulieu et al. 2013; Beaulieu and O'Meara 2016), although Gamble et al. (2017) dispute these results due to potentially high Type 1 error rates (Davis et al. 2013; Maddison and FitzJohn 2015; Rabosky and Goldberg 2015). Future studies may want to consider incorporating character-state correlated diversification information into ancestral state reconstructions using the recently published nonparametric FiSSE (Fast, intuitive, State-dependent, Speciation-Extinction) approach (Rabosky and Goldberg 2017; Zenil-Ferguson and Pennell 2017).

When considering other lines of evidence such as the variation in toe hyperextension anatomy within geckos (Russell 1979), it is likely that the true number of origins within geckos lies somewhere between one and many (Gamble et al. 2017). Future studies investigating the origins of adhesive toe pads in lizards will benefit from considering multiple lines of evidence (Gamble et al. 2017). The adhesive toe pads of lizards vary in toe pad shape, spinule/seta morphology, skin-to-bone digital tendon system characteristics (Russell 2002), and the presence/absence of internal blood sinuses and paraphalanges (Russell 1976; Russell and Bauer 1988; Gamble et al. 2012). The presence of epidermal spinules may predispose lizards to express adhesive setae, with epidermal spinules having likely evolved into adhesive setae (Maderson 1970; Stewart and Daniel 1972; Russell 1976; Peterson 1983; Peattie 2008). Epidermal spinules appear to be common across geckos and other lizards, including Chamaeleonidae, Iguanidae, Leiocephalidae, and Polychrotidae (Maderson 1964; Ruibal 1968; Maderson 1970; Stewart and Daniel 1975; Peterson 1984; Bauer and Russell 1988; Irish et al. 1988; Peattie 2008; Vucko 2008). Russell et al. (2015) provide a stunning example in *Gonatodes,* highlighting variation in

both setal and toe pad morphology suggesting that *Gonatodes* may represent an example of elongated spinules and enlarged ventral scales performing as a friction-generating pad.

Trait Evolution

We used angle of toe detachment as a measure of adhesive performance because it has a well-supported mechanistic basis (Autumn et al. 2006a; Tian et al. 2006), although other metrics exist (Irschick et al. 1996; Irschick et al. 2006; Stark et al. 2012; Crandell et al. 2014). Using this measure of performance, we saw striking differences between our focal clades. Species with the lowest detachment angles (mostly anoles, near 15°) only produce a maximum of 0.27 units of adhesion for one unit of friction, [using *tangent*(detachment angle) = adhesion/friction (Autumn et al. 2006a; Hagey et al. 2014)], whereas our best performing species, with detachment angles over 40°, particular Gekkonidae geckos, can produce up to 0.84 units of adhesion for every unit of friction, over three times as much as our lowest performing species.

Our modified models of trait evolution, which relied on results from our ancestral state reconstruction providing evidence that the ancestors of geckos and anoles lacked toe pads, found that gecko performance is well described by a BM with a trend model or a weak OU model with parameters converging towards a BM with a trend (large σ^2, distant θ, and small α values; Table 1; Fig. 4, 5) suggesting adhesive performance in geckos has evolved directionally, yet unbounded. Conversely, our results suggest anoles, which are much younger than geckos, evolved rapidly in a bounded sub-section of performance space, similar to a conventional stabilized OU model (short phylogenetic half-life and a θ value near observed values; Table 1; Fig. 4, 5), but due to our limited sampling of anoles we could not rule out a Brownian Motion with a trend model.

These observed differences in performance and evolutionary tempo and mode mirror anole and gecko macro- and micro-adhesive morphology, ecology, and the fossil record. For example, geckos were found to be more variable in adhesive performance (Fig. 3) and also have a much wider range of toe pad shapes, setal morphology (Peattie 2007; Gamble et al. 2012), and ecology as compared to anoles. Geckos live in tropical, arid, and temperate environments on rocks, vegetation, and terrestrial substrates, whereas anoles are generally found in arboreal microhabitats in the Caribbean and South America. Mainland anoles have more detachment angle diversity as compared to Caribbean anoles. These differences may be related to mainland

and Caribbean lizard community structure and ecological opportunity (Macrini et al. 2003; Losos 2009). As a result, geckos may be evolving within many different adaptive zones, while the limited variation in the ecology of anoles may be driving them towards one or a few adaptive zones without selecting for novel adhesive morphology. Further work exploring the relationship between adhesive performance and habitat use of padded lizards is also crucial to place performance reported here in an ecological context. Conversely, the evolvability of the gecko and anole adhesive systems may be a driving factor, allowing geckos to diversify extensively, and limiting anole toe pad shape, setal morphology, or performance and hence limiting them to one or few adaptive zones. Our trait modeling results also complement studies of the fossil record. Studies of trait evolution can sometimes underestimate ancestral trait diversity (Mitchell 2015), but recent fossil evidence from anoles preserved in amber suggests a model in which anoles rapidly evolved their current phenotypes, with anole ecomorphs having changed little since the Miocene (Sherratt et al. 2015). The gecko fossil record is unfortunately less informative (Daza et al. 2014; Daza et al. 2016).

Our results provide an example of convergent traits evolving under different evolutionary histories, highlighting the importance of considering macroevoutionary dynamics to infer historical contingency and ecological opportunity during adaptation and evolution and considering the evolution of performance instead of morphological traits. Despite our results detailing strong evolutionary constraints on anole evolution that we did not find in geckos, there remain many open questions as to how lizard adhesive toe pads have evolved, how they work, and how they are used in the wild. Our results highlight the need to conduct more biomechanical, ecological, and developmental studies of padded lizards with an explicit consideration of their origins. Our results also illustrate the value in incorporating additional information into comparative phylogenetic methods. Without the use of our modified *bayou* model, we would not have identified differences between the evolution of performance in geckos and anoles and we strongly encourage researchers to investigate their model assumptions.

Acknowledgements

We would like to thank the National Science Foundation in collaboration with Aaron Bauer and Todd Jackman (Award #0844523), the National Geographic Society/Waitts Institute (Grant

#W216-12), the BEACON Center for the Study of Evolution in Action (Request #302, #429), the NSF Collaborative Research grant: Arbor: Comparative Analysis Workflows for the Tree of Life (Harmon et al. 2013), and Sigma XI (#G200803150489) for funding, Matt Pennell for helpful discussions, Jon Eastman for help with analyses, Jon Boone for access to animals, Bobby Espinoza, JR Wood, Jesse Grismer, Mat Vickers, Andrew Schnell, Scott Harte, Alyssa Stark, Peter Niewiarowski, Ali Dhinojwala, Jonathan Losos, Anthony Herrel, Shane Campbell-Staton, Kristi Fenstermacher, Hannah Frank, Martha Munoz, and Paul VanMiddlesworth for help collecting data in the lab and field, and multiple editors and anonymous reviewers for helpful comments. None of the authors declare any conflicts of interest.

Data Accessibility

See Supplemental Material

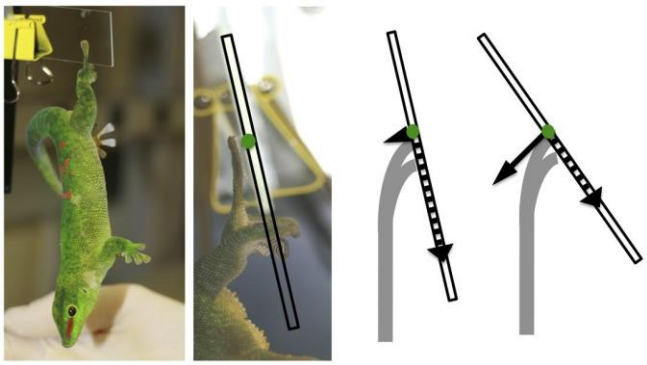

Figure 1. Angle of Toe Detachment Assay. To quantify toe detachment angle, a pad bearing lizard is suspended from a glass microscope slide by a single rear toe (left images). When the glass substrate is near vertical, the lizard's toe pad, and hence setae, are predominantly generating friction relative to the substrate (see right images, seta illustrated in gray, friction illustrated as dotted arrows). As the substrate is slowly inverted, the setae generate relatively less friction and more adhesion (see far right image, adhesion illustrated as solid arrow). At the angle of toe detachment, the setae can no longer maintain the proper orientation with the substrate to remain attached and the animal falls onto a cushioned base (see video links in Supplemental Material). As a result, the angle of toe detachment quantifies the maximum amount of adhesion, relative to friction, generated. Image modified from Hagey et al. (2014).

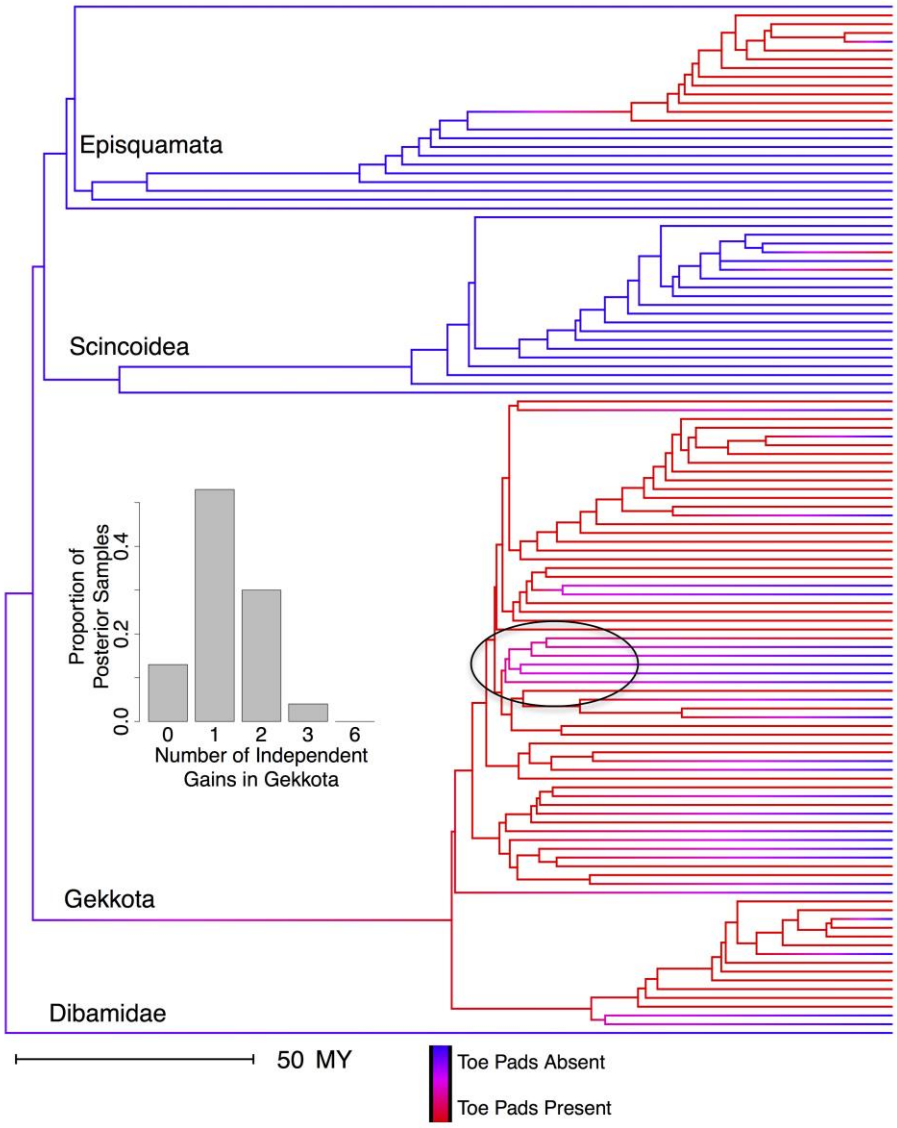

Figure 2. Toe Pad Ancestral State Reconstruction. We reconstructed the presence (red) and absence (blue) of adhesive toe pads across Squamata. We predicted toe pads likely evolved once within geckos, with many losses. The embedded histogram highlights the number of independent origins within Gekkota across our posterior sample of reconstructions (see Methods). Some of the reconstructions in our posterior sample yielded independent origins of toe pads in the stem leading to *Hemidactylus* (see Results). The root of the clade containing *Hemidactylus* is circled. For tip names see Supplemental Material.

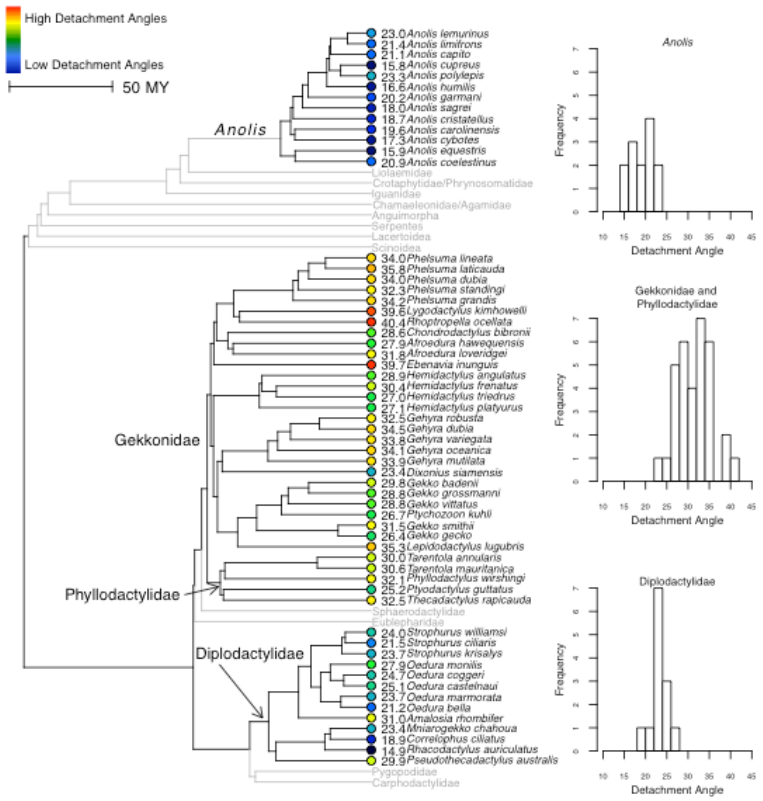

Figure 3. Phylogeny of Focal Padded Species with Performance Data. We quantified toe-detachment angle across 46 species of geckos and 13 species of anoles. Colored circles and numbers at the tips of the phylogeny represent each species' estimated detachment angle. Warmer colors represent higher detachment angles. We display prominent non-padded lizard groups to emphasize the evolutionary distance between anoles and geckos and to highlight the fact that not all families of geckos have toe pads (Carphodactylidae and Eublepharidae lack pads, Pygopodidae lacks limbs). Sphaerodactyls do possess adhesive toe pads, but we did not quantify their performance. Histograms to the right of the phylogeny illustrate the observed variation in performance within anoles, diplodactyls, and gekkonids and phyllodactylids. We found *Anolis* lizards to have the lowest detachment angles, followed by diplodactylids. Gekkonids and phyllodactylids had the highest and broadest range of detachment angles.

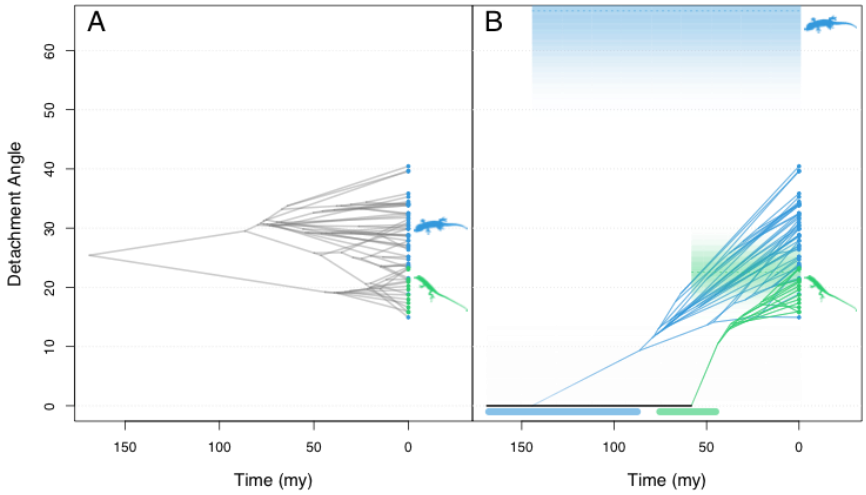

Figure 4. Ancestral state reconstructions using a single-regime BM model (A) and the median posterior parameter estimates for the *OU$\sigma^2\alpha\theta_{Bayesian}$ model (B) in *bayou*, which assumes independent origins of toe pads geckos and anoles. Anole data are displayed in green and gecko data in blue. B) median parameter estimates for the OU target value are indicated by colored dotted lines within the shaded bands indicating the expected densities of the stationary distributions. Horizontal bars below the X-axis indicate the constrained shift regions. Note the median predicted ancestral performance in plot A is estimating a toe detachment angle of approximately 25° for the shared ancestor of geckos and anoles, which likely lacked toe pads. See Supplemental Material for additional analyses assuming two origins of toe pads in Gekkota.

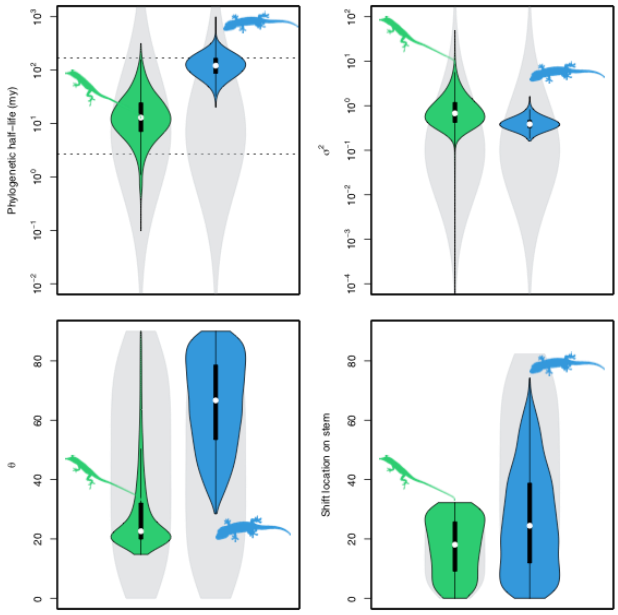

Figure 5. Posterior distributions from the *OU$\sigma^2\alpha\theta_{Bayesian}$ model. Anole data are displayed in green on the left of each plot. Gecko data are in blue on the right of each plot. White dots indicate median estimates for each parameter while black rectangles and whiskers indicate quartiles of the distribution. Gray violin plots indicate the prior distribution. The upper dotted line on the phylogenetic half-life plot indicates the root age of the Squamata phylogeny corresponding roughly to the value at which the OU model approaches a Brownian Motion model. The lower dotted line represents the value of phylogenetic half-life at which no two species in either phylogeny would have more than a 0.05% phylogenetic correlation, *i.e.*, the values at which our model simplifies into a white-noise model with independent, identically distributed trait values with no effect of phylogeny.

OU/wic Models	AICc Weights	Parameter Values			
		Root	σ^2		
BM1	0.35	25.5	0.28		
		θ	σ^2	ln(2)/α	
OU/σ^2/α	0.19	19.0	0.46	22.2	Anoles
		>90.0	3.56	>1000	Geckos
		θ	σ^2	ln(2)/α	
OU0	0.13	19.0	0.33	161.7	Anoles
		32.7			Geckos
		Root	σ^2		
BMσ^2	0.12	25.5	0.28		Anoles
			0.28		Geckos
		θ	σ^2	ln(2)/α	
OU1	0.12	25.5	0.28	>1000	
		θ	σ^2	ln(2)/α	
OUα0	0.05	18.9	0.42	100.8	Anoles
		43.6		390.4	Geckos
		θ	σ^2	ln(2)/α	
OU$\sigma^2$0	0.05	18.9	0.29	114.0	Anoles
		32.4	0.39		Geckos

BAYOU Models	AICc Weights	Parameter Values					
		Root/θ	σ^2	ln(2)/α	μ	Shift Time	
*BMT$_{\sigma^2}$-OU$_{\alpha}$	0.37	19.4	29.7	0.3	--	32.2	Anoles
		0.0	0.27	--	0.35	82.3	Geckos
		Root	σ^2	ln(2)/α	μ	Shift Time	
*BMT	0.34	0.0	0.27	--	0.34	25.4	Anoles
						82.3	Geckos
		Root	σ^2	ln(2)/α	μ	Shift Time	
*BMTμ	0.18	0.0	0.27	--	0.43	32.2	Anoles
					0.35	82.3	Geckos
		θ	σ^2	ln(2)/α	μ	Shift Time	
*OU$\sigma^2\alpha$0	0.04	19.4	52.1	0.2	--	22.9	Anoles
		90.0	0.33	208.2		25.6	Geckos
		θ	σ^2	ln(2)/α	μ	Shift Time	
*OU1	0.04	90.0	0.36	117.6	--	18.3	Anoles
						49.9	Geckos
		θ	σ^2	ln(2)/α	μ	Shift Time	
*OU0	0.02	90.0	0.36	117.6	--	18.3	Anoles
		90.0				49.9	Geckos
		θ	σ^2	ln(2)/α	μ	Shift Time	
*OUα0	0.01	90.0	0.41	2.3	--	21.4	Anoles
		90.0		98.9		55.3	Geckos
		θ	σ^2	ln(2)/α	μ	Shift Time	
*OU$\sigma^2$0	0.01	90.0	0.30	98.9	--	21.4	Anoles
		90.0	0.41			55.3	Geckos
		Root	σ^2	ln(2)/α	μ	Shift Time	
*BM1	0.00	0.0	0.59	--	0.00	0.0	Anoles
						0.0	Geckos
		θ	σ^2	ln(2)/α	μ	Shift Time	
*OU$\sigma^2\alpha\theta_{\text{Anoles}}$	--	22.6 (17.2, 61.1)	0.68 (0.00, 3.08)	12.9 (0.1, 65.4)	--	18.1 (1.9, 32.2)	Anoles
		66.7 (39.2, 90.0)	0.39 (0.22, 0.66)	121.5 (37.1, 247.7)		24.5 (0.0, 57.2)	Geckos

564

Table 1. Model of Trait Evolution Fits and Estimated Parameters. We evaluated multiple models of trait evolution using the OUwie, and *bayou* packages. We ascribed model names based on their use of a BM or OU procedure followed by parameters that were allowed to vary across clades. We display AICc weights and parameter estimates for each model we considered, sorted by their AICc weights. The models considered in our *bayou* analyses all incorporated constraints (denoted by asterisks) limiting the trait value to 0° prior to the stem branches leading to geckos and anoles. We report the predicted timing of the origins of toe pads in geckos and anoles (Shift Time) in millions of years since the split of the stem segregating the clade from the rest of the phylogeny. OU α values are displayed as phylogenetic half-life values ($ln[2]/\alpha$) in millions of years. Our *bayou* Brownian Motion models also include root parameter values illustrating the trait value at the root of the phylogeny. In BM models lacking a trend, in which the μ parameter is zero, the root parameter value is also the clade mean. The μ parameter represents the expected change in trait over time. Lastly, results from our *$OU\sigma^2\alpha\theta_{Bayesian}$ model included estimated medians and 95% highest posterior density (HPD) intervals for each parameter, indicated in parentheses under each value, displayed in the last row of the table.

Supplemental Material

Here we provide additional information including species level data, links to performance assay videos, additional results, and a description of how we measured performance in the field using purpose-built equipment.

File S.1. A .xlsx file listing our toe pad presence/absence assignments for all 4162 tips in the squamate phylogeny from Pyron and Burbrink (2013).

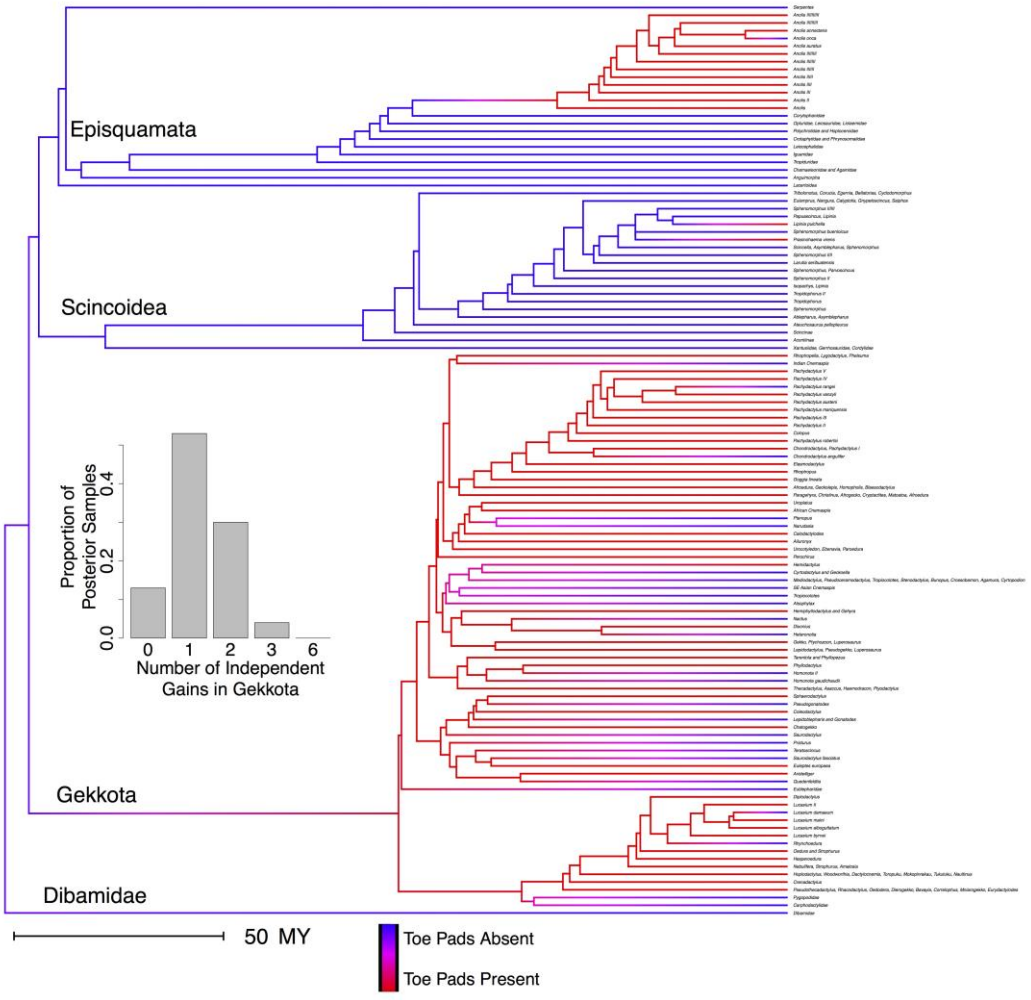

Figure S.1 Ancestral State Reconstruction with Tip Names (see Figure 2, Methods, and Results for additional information)

Modeling Trait Evolution Assuming Two Origins of Toe Pads within Gekkota

In addition to analyses assuming a single origin of toe pads within geckos, we considered an additional set of limited analyses assuming two independent origins of toe pads within Gekkota, one origin at the base of the Diplodactylidae family and a second at the base of the Phyllodactylidae and Gekkonidae clade. Our primary goal with these analyses was to determine whether two origins (which received some support in our reconstruction of toe pad evolution) changed our primary conclusions —namely, that Gekkota evolved under BM-like evolution with a trend with limited evidence of constraint.

Models fit to two-origin scenarios recover very similar dynamics, with Brownian motion with a trend being preferred over an OU model (AICs: BM with a trend = 264.3; OU = 296.3). Furthermore, even when an OU model is fit to our two gecko clades, they recover very BM-like dynamics with long phylogenetic half-lives (Gekkonidae/Phyllodactylidae = 136.7 my; Diplodactylidae = 193.0 my). Furthermore, we find little evidence for unique dynamics between the two putative origins (AICs: OU shared parameters = 297.4; OU independent parameters = 296.3), suggesting that the two gecko clades generally evolve under similar dynamics. We visualized our analysis by fitting the OU model described above in a Bayesian framework (left plot) with separate origins for Diplodactylidae (purple) and other Gekkonidae/Phyllodactylidae (blue). Both clades had long half-lives (Gekkonidae/Phyllodactylidae median = 91.5 my; Diplodactyline median = 64.8 my) and distant optima (Gekkonidae/Phyllodactylidae median [95%CI] = 67.6° [33.3°, 88.8°]; Diplodactyline geckos median [95%CI] = 46.1° ° [23.5°, 87.3°]). We compared this model to our Bayesian model from the main text (right plot). Note that although BM with a trend was preferred over OU models, OU models with distant optima and long phylogenetic half-lives approximate BM with a trend. As in the main text, we set uniform priors on the location of the optima to be less than or equal to 90°. We conclude that even with multiple origins, the data suggest more gradual and unconstrained trait evolution across the geckos than in the *Anolis* lizards.

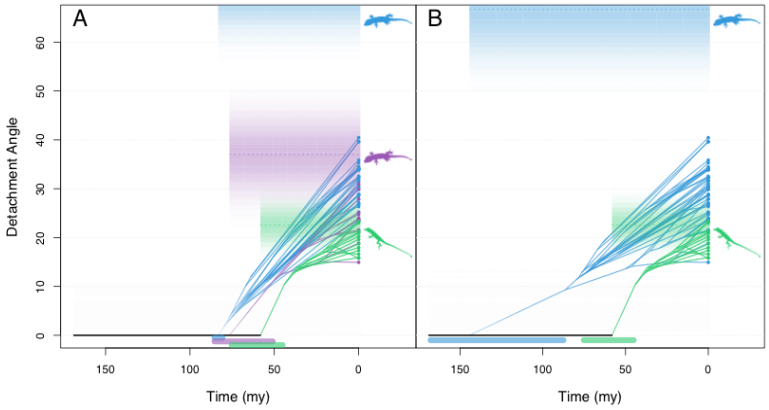
A
B
Detachment Angle
0
10
20
30
40
50
60
150
100
50
0
Time (my)
Time (my)

619

620

621

Species	Clade	Species Mean Detachment Angle and Variance	Number of Individuals Observed
Anolis capito	*Anolis*	21.09 (0.43)	NA
Anolis carolinensis	*Anolis*	19.62 (0.81)	6
Anolis coelestinus	*Anolis*	20.89 (0.06)	3
Anolis cristatellus	*Anolis*	18.71 (0.71)	7
Anolis cupreus	*Anolis*	15.77 (0.31)	NA
Anolis cybotes	*Anolis*	17.35 (0.79)	3
Anolis equestris	*Anolis*	15.91 (0.76)	1
Anolis garmani	*Anolis*	20.21 (0.44)	1
Anolis humilis	*Anolis*	16.61 (0.38)	NA
Anolis lemurinus	*Anolis*	23.04 (0.41)	NA
Anolis limifrons	*Anolis*	21.37 (0.51)	NA
Anolis polylepis	*Anolis*	23.27 (0.28)	NA
Anolis sagrei	*Anolis*	17.96 (0.78)	7
Amalosia rhombifer	Diplodactylidae	30.96 (0.33)	6
Correlophus ciliatus	Diplodactylidae	18.85 (0.22)	3
Mniarogekko chahoua	Diplodactylidae	23.43 (0.12)	6
Oedura castelnaui	Diplodactylidae	25.13 (0.80)	4
Oedura coggeri	Diplodactylidae	24.72 (0.02)	4
Oedura marmorata	Diplodactylidae	23.68 (0.82)	4
Oedura monilis	Diplodactylidae	27.87 (0.45)	3
Oedura bella	Diplodactylidae	21.24 (1.76)	1
Pseudothecadactylus australis	Diplodactylidae	29.91 (1.00)	2
Rhacodactylus auriculatus	Diplodactylidae	14.93 (0.54)	2
Strophurus ciliaris	Diplodactylidae	21.54 (0.25)	4
Strophurus krisalys	Diplodactylidae	23.68 (2.02)	7
Strophurus williamsi	Diplodactylidae	24.02 (0.35)	1
Afroedura hawequensis	Gekkonidae and Phyllodactylidae	27.89 (0.31)	6
Afroedura loveridgei	Gekkonidae and Phyllodactylidae	31.77 (0.88)	5
Chondrodactylus bibronii	Gekkonidae and Phyllodactylidae	28.57 (0.41)	3
Dixonius siamensis	Gekkonidae and Phyllodactylidae	23.38 (0.71)	3
Ebenavia inunguis	Gekkonidae and Phyllodactylidae	39.71 (0.08)	4
Gehyra dubia	Gekkonidae and Phyllodactylidae	34.48 (0.31)	8
Gehyra mutilata	Gekkonidae and Phyllodactylidae	33.85 (1.36)	7
Gehyra oceanica	Gekkonidae and Phyllodactylidae	34.15 (1.88)	3
Gehyra robusta	Gekkonidae and Phyllodactylidae	32.50 (0.98)	7
Gehyra variegata	Gekkonidae and Phyllodactylidae	33.84 (0.33)	8
Gekko badenii	Gekkonidae and Phyllodactylidae	29.84 (1.19)	6
Gekko gecko	Gekkonidae and Phyllodactylidae	26.36 (0.14)	13
Gekko grossmanni	Gekkonidae and Phyllodactylidae	28.77 (0.12)	2
Gekko smithii	Gekkonidae and Phyllodactylidae	31.49 (0.97)	5
Gekko vittatus	Gekkonidae and Phyllodactylidae	28.77 (0.62)	2
Hemidactylus angulatus	Gekkonidae and Phyllodactylidae	28.88 (0.43)	4
Hemidactylus frenatus	Gekkonidae and Phyllodactylidae	30.37 (2.04)	4
Hemidactylus platyurus	Gekkonidae and Phyllodactylidae	27.12 (3.35)	9
Hemidactylus triedrus	Gekkonidae and Phyllodactylidae	26.96 (0.50)	4
Lepidodactylus lugubris	Gekkonidae and Phyllodactylidae	35.29 (0.33)	6
Lygodactylus kimhowelli	Gekkonidae and Phyllodactylidae	39.58 (1.31)	5
Phelsuma dubia	Gekkonidae and Phyllodactylidae	34.02 (0.43)	4
Phelsuma grandis	Gekkonidae and Phyllodactylidae	34.19 (0.16)	5
Phelsuma laticauda	Gekkonidae and Phyllodactylidae	35.85 (0.13)	5
Phelsuma lineata	Gekkonidae and Phyllodactylidae	33.96 (0.21)	5
Phelsuma standingi	Gekkonidae and Phyllodactylidae	32.30 (0.70)	7
Phyllodactylus wirshingi	Gekkonidae and Phyllodactylidae	32.13 (0.61)	4
Ptychozoon kuhli	Gekkonidae and Phyllodactylidae	26.66 (1.85)	2
Ptyodactylus guttatus	Gekkonidae and Phyllodactylidae	25.20 (2.71)	8
Rhoptropella ocellata	Gekkonidae and Phyllodactylidae	40.45 (0.52)	6
Tarentola annularis	Gekkonidae and Phyllodactylidae	29.97 (1.13)	2
Tarentola mauritanica	Gekkonidae and Phyllodactylidae	30.57 (0.25)	3
Thecadactylus rapicauda	Gekkonidae and Phyllodactylidae	32.53 (0.43)	4

Table S.1. Performance Observations. Species mean toe detachment angle and variance (displayed in parentheses). The number of individuals tested was not recorded for some species of anoles (number of individuals = NA) and were treated as observations from a single individual in our analyses.

File S.2 Performance Observations .xlsx file

Links illustrating our toe detachment assay on YouTube:

Far away view: https://www.youtube.com/watch?v=4EDUi9If-4c

Close up view: https://www.youtube.com/watch?v=HC-FdtGqv54

AUTEUR and SURFACE Analyses

In addition to our OUwie and modified *bayou* trait evolution analyses, we also considered BM trait evolution using AUTEUR (Eastman et al. 2011), currently within the *geiger* package, and shifts in the OU target parameter θ (assuming α, the strength of pull towards θ, and the rate of diffusion, σ^2, are shared across clades) using the R package SURFACE (Ingram and Mahler 2013). These analyses each require different *a priori* information and use different model fitting approaches. AUTEUR does not require *a priori* clade assignments and uses a reversible-jump MCMC approach to fit multi-regime BM models, allowing either the rate of change (σ^2), mean trait value (θ), or both parameters to vary between clades. We evaluated models with clade specific σ^2 values (BMσ^2), clade specific θ values (BMθ), and models in which both θ and σ^2 could vary (BM$\sigma^2\theta$), all while including species-level trait value error. For each dataset, we conducted two runs, evaluating chain convergence. All of our AUTEUR runs used one million generations, sampling every five hundred generations.

The SURFACE package uses a step-wise AIC approach without *a priori* clade assignments, varying the OU parameter θ for different clades until the AIC score can no longer be improved. This package was designed to identify examples of convergence and so the second phase of the analysis condenses previously identified regimes, allowing parameter values to be shared between clades, and reducing the total number of unique parameter sets. We conducted simulations to determine if the model identified by SURFACE contained a significant number of regimes as compared to the number expected by chance under a single-rate BM model. We simulated 500 datasets under BM using our cropped Pyron and Burbrink (2013) phylogeny. We ran each simulated dataset through the forward and backward phases of SURFACE and tabulated the number of regimes observed to generate a null distribution.

The results from our AUTEUR analyses, which considered multi-rate and multi-theta BM models, found no significant changes in rate or mean across clades. All six of our runs, varying σ^2 (BMσ^2), θ (BMθ), or σ^2 and θ concurrently (BM$\sigma^2\theta$) with two replicates each, estimated similar parameter values ($\sigma^2 = 0.29 \pm 0.005$ SE, $\theta = 25.6 \pm 0.03$ SE, see Table below). We display σ^2 and θ parameter estimates for each of our duplicate simulations (denoted as subscript one or two). We concluded that our duplicate runs were converging by comparing σ^2 and θ posterior probabilities of each branch between duplicated runs, finding them to be similar. We also used the Heidelberger and Welch convergence diagnostic, which includes the Cramer-von-

Mises statistic and the half-width test. In all of our analyses, the root and log-likelihood parameters passed both tests. We found effective sizes ranging from 598 to 2104 for our root and log-likelihood parameters across all our runs, which take into account autocorrelation between successive MCMC chain samples.

AUTEUR

Models	σ^2	θ
$BM\theta_1$	0.31	25.5
$BM\theta_2$	0.31	25.5
$BM\sigma^2_1$	0.29	25.6
$BM\sigma^2_2$	0.29	25.7
$BM\sigma^2\theta_1$	0.28	25.6
$BM\sigma^2\theta_2$	0.29	25.6

Our SURFACE analyses originally found a multi-θ OU model with five regimes condensed into four made up of anoles and diplodactylid geckos, gekkonids and phyllodacylids, *Rhacodactylus auriculatus*, and three gekkonid species, *Lygodactylus kimhowelli*, *Rhoptropella ocellata*, and *Ebenavia inunguis*, Below we display parameter estimates and AIC scores for single-regime BM and OU (BM1 and OU1), and uncondensed and condensed models. During the stepwise SURFACE analysis our model AIC scores dropped as more regimes were added (black triangles; see Figure and Table below), starting at a single-theta OU model (upper dotted line, AIC = 338.9), until the analysis settled on a five-regime model (AIC = 330.9), scoring lightly better than a single-regime BM model (lower dashed line, AIC = 332.5). The analyses then looked for improvements to the AIC score by condensing regimes. By condensing the two small regimes within Gekkonidae into one, the AIC score and number of unique regimes were reduced to four and an AIC of 327.7. Although, when we consider the number of regimes expected under a single-rate BM model, we see that five regimes with one condensation event could easily occur by chance. In our 500 simulated datasets under single-rate BM, we found an average of 5.3 regimes, a mode of five, and a maximum of 11 regimes, with an average of 2.0 convergence events, a mode of two, and a maximum of six convergence events. These simulations suggest that a multi-theta OU model like the one we observed fitting our data best may have a low AIC score (327.7), but it is a pattern that can easily appear under a single-rate BM model (AIC = 332.5).

Considering the fact that our SURFACE analyses successfully fit divergent species to their own regimes (*Rhacodactylus auriculatus*, *Lygodactylus kimhowelli*, *Rhoptropella ocellata*,

and *Ebenavia inunguis*), we conducted a further analysis, manually condensing high performing diplodacylid geckos (*Amalosia rhombifer* and *Pseudothecadactylus australis*) into the gekkonid regime and recalculated the AIC score for this new, further condensed, model (red triangles; see Figure and Table below). We found our uncondensed seven-regime model had a higher AIC (331.9) as compared to the non-condensed five-regime model SURFACE found, yet when we condensed our modified model into four regimes, its AIC score (322.3) dropped well below the best condensed four-regime model identified by SURFACE. We believe this model was not chosen by the initial SURFACE analysis due the stepwise AIC approach SURFACE uses.

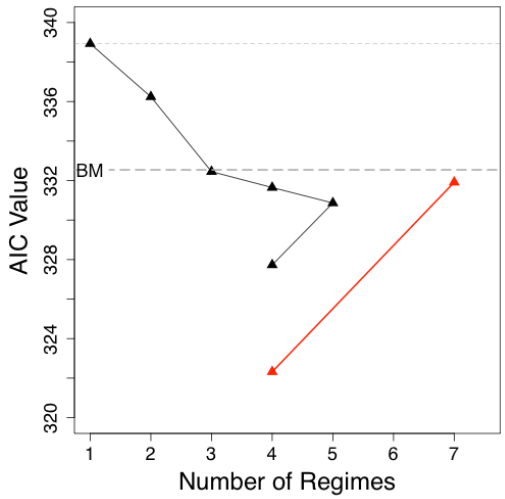

SURFACE Models	AIC	σ^2	α	θ
BM1	332.54	0.29	NA	25.4
OU1	338.93	0.33	0.003	25.7
$OU\theta_{Uncondensed}$	330.86	0.33	0.013	22.1 - *Anolis*, Diplodacylidae 33.2 - Gekkonidae, Phyllodactylidae 49.3 - *Lygodactylus, Rhoptropella* -8.2 - *Rhacodactylus* 48.1 - *Ebenavia*
$OU\theta_{Condensed}$	327.73	0.33	0.013	22.1 - *Anolis*, Diplodacylidae 33.2 - Gekkonidae, Phyllodactylidae 48.8 - *Lygodactylus, Rhoptropella, Ebenavia* -8.2 - *Rhacodactylus*
$OU\theta_{Modified\ Uncondensed}$	331.91	0.31	0.016	20.8 - *Anolis*, Diplodacylidae 33.0 - Gekkonidae, Phyllodactylidae 47.0 - *Lygodactylus, Rhoptropella* -0.3 - *Rhacodactylus* 46.0 - *Ebenavia* 39.7 - *Amalosia* 36.0 - *Pseudothecadactylus*
$OU\theta_{Modified\ Condensed}$	322.32	0.34	0.018	20.7 - *Anolis*, Diplodacylidae 32.8 - Gekkonidae, Phyllodactylidae, *Amalosia, Pseudothecadactylus* 45.5 - *Lygodactylus, Rhoptropella, Ebenavia* 1.2 - *Rhacodactylus*

Measuring Performance in the Field

Pad bearing lizards with higher detachment angles can likely use highly angled or inverted perches more easily, whereas species with lower detachment angles likely struggle to generate as much adhesion relative to friction and thus may be limited to vertical perches, although toe orientation and foot shape likely play a large role in inverted locomotion. In addition, there may exist a trade-off in high and low detachment angles regarding the production of friction versus adhesion. Species with a high detachment angle likely have setae and spatulae shaped to maintain proper contact with a substrate under high setal shaft angles, producing some amount of both adhesion and friction, but less absolute friction than if the setal shaft angle was near parallel with the substrate, translating the applied force into only friction (also see Pesika et al. 2007). Additional research considering the setal mechanics underlying detachment angle would be necessary to further describe this potential trade-off. In addition, rough surfaces offer a reduced surface area for a padded lizard to attach to, and as a result, higher detachment angles may allow setae to properly attach to the valleys and peaks of a rough surface (Sitti and Fearing 2003; Gillies and Fearing 2014; Gillies et al. 2014).

As part of this study, gecko performance was collected in Queensland, Australia using purpose-built equipment consisting of a Pacific Scientific Powermax 1.8° stepper motor (model #P21NRXB-LNN-NS-00), Vernier dual-range force sensor, Vernier three-axis accelerometer, Vernier sensorDAQ data-acquisition interface, and a Phidget bipolar stepper control board (#1063_1). Operation and data collection used a custom LabVIEW program (2011 version 11.0.1f2, National Instruments, Austin, TX, USA) running on a Gateway LT series netbook (LT2805u). The frame of our toe detachment equipment was custom-built and acted as a lever with a fulcrum in the center, force sensor at one end, and the lizard suspended from the other end (Fig. S.2).

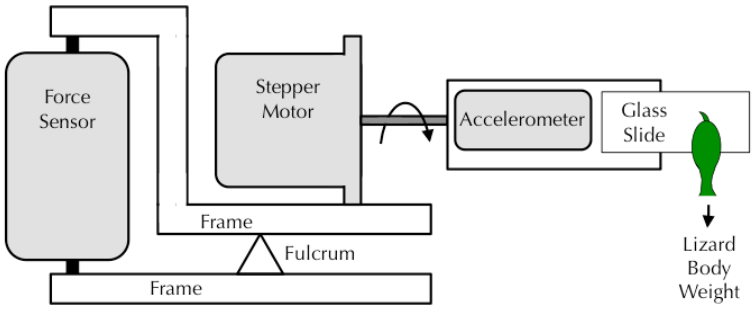

Figure S.2. Toe Detachment Field Equipment. We build a field-capable TAD device consisting of a force sensor, stepper motor, and multi-axis accelerometer. The upper frame of our apparatus acts as a lever with the fulcrum, allowing the force sensor (left side of image) to detect when a lizard detaches from the glass (right side of image). Our glass slide and accelerometer were attached to a large flat plate. The accelerometer was positioned to measure acceleration in the Y direction (vertical in our image) and Z direction (perpendicular to the mounting surface, out of the plane of the image, towards the reader).

An accelerometer, attached to the rotating glass surface, allowed us to determine the angle of the glass surface throughout the course of each trial. Raw toe detachment data consisted of three variables recorded over the course of each trial (acceleration in Y and Z directions and force). By calculating the arctangent of the ratio of the two acceleration measurements perpendicular to the axis of rotation, we could determine angle (Fig. S.2). When rotating, acceleration due to gravity was not linear; rather it changed slowly when near vertical. When near horizontal, acceleration due to gravity changed quickly.

Our force sensor recorded the corresponding change in force (Fig. S.3) and allowed us to pinpoint the instant the lizard detaches during a trial. We fit a three-parameter broken regression model to our force output data to pinpoint the moment the lizard detached (Fig. S.3). We estimated the y-intercept of a horizontal line fit to the force data before the lizard fell, the time point at which the lizard fell, and the y-intercept of a horizontal line fit to the force data after the lizard detached (Fig. S.3). Using our estimated time of detachment and our angle data (calculated from accelerometer data), we estimated the angle of the glass at the time of detachment (Fig. S.3).

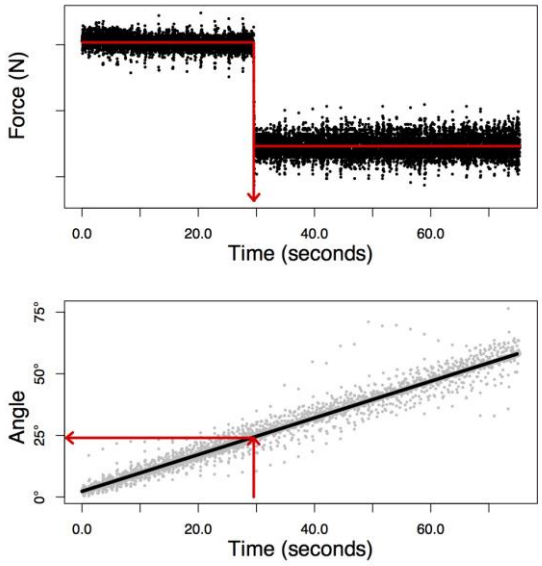

Figure S.3. Representative Toe Detachment Performance Trial. Representative data output from a single toe detachment trial is displayed. Time is on the X-axis. Raw force data (upper plot) displays our two estimated y-intercepts (red horizontal lines) and time of detachment (red vertical line, approximately 30 seconds in this example) estimated by a broken regression analysis. Raw acceleration data were used to estimate the angle of the glass slide through time (lower plot, gray points). The black line in our lower plot is the estimated substrate angle over the course of the trial. Our estimated angle of toe detachment is the point in which our estimated time of detachment intersects with our estimated angle, slightly under 25° in this example.

Work Cited

Arnold, S. J. 1983. Morphology, performance and fitness. Am Zool 23:347-361.

Austin, C. C. 1998. Phylogenetic relationships of *Lipinia* (Scincidae) from New Guinea based on DNA sequence variation from the mitochondrial 12S rRNA and nuclear c-mos genes. HAMADRYAD-MADRAS- 23:93-102.

Autumn, K., A. Dittmore, D. Santos, M. Spenko, and M. Cutkosky. 2006a. Frictional adhesion: a new angle on gecko attachment. J. Exp. Biol. 209:3569-3579.

Autumn, K., S. T. Hsieh, D. M. Dudek, J. Chen, C. Chitaphan, and R. J. Full. 2006b. Dynamics of geckos running vertically. J. Exp. Biol. 209:260-272.

Autumn, K., P. H. Niewiarowski, and J. B. Puthoff. 2014. Gecko adhesion as a model system for integrative biology, interdisciplinary science, and bioinspired engineering. Annu Rev Ecol Evol S 45:445-470.

Bauer, A. M. 1998. Morphology of the adhesive tail tips of carphodactyline geckos (Reptilia: Diplodactylidae). J Morphol 235:41-58.

Bauer, A. M. and A. P. Russell. 1988. Morphology of gekkonid cutaneous sensilla, with comments on function and phylogeny in the Carphodactylini (Reptilia: Gekkonidae). Can. J. Zool 66:1583-1588.

Beaulieu, J. M., D. C. Jhwueng, C. Boettiger, and B. C. O'Meara. 2012. Modeling Stabilizing Selection: Expanding the Ornstein-Uhlenbeck Model of Adaptive Evolution. Evolution 66:2369-2383.

Beaulieu, J. M. and B. C. O'Meara. 2016. Detecting Hidden Diversification Shifts in Models of Trait-Dependent Speciation and Extinction. Syst Biol 65:583-601.

Beaulieu, J. M., B. C. O'Meara, and M. J. Donoghue. 2013. Identifying hidden rate changes in the evolution of a binary morphological character: the evolution of plant habit in campanulid angiosperms. Syst Biol 62:725-737.

Brown, D., J. W. Wilmer, and S. Macdonald. 2012. A revision of *Strophurus taenicauda* (Squamata; Diplodactylidae) with the description of two new subspecies from central Queensland and a southerly range extension. Zootaxa:1-28.

Burnham, K. P. and D. R. Anderson. 2002. Model selection and multi-model inference: a practical information-theoretic approach. Springer, New York, NY.

794 Butler, M. A. and A. A. King. 2004. Phylogenetic comparative analysis: A modeling approach
795 for adaptive evolution. Am. Nat. 164:683-695.
796 Crandell, K. E., A. Herrel, M. Sasa, J. B. Losos, and K. Autumn. 2014. Stick or grip? Co-
797 evolution of adhesive toepads and claws in *Anolis* lizards. Zoology 117:363-369.
798 Davis, M. P., P. E. Midford, and W. Maddison. 2013. Exploring power and parameter estimation
799 of the BiSSE method for analyzing species diversification. Bmc Evol Biol 13.
800 Daza, J. D., A. M. Bauer, and E. D. Snively. 2014. On the fossil record of the Gekkota. Anat Rec
801 (Hoboken) 297:433-462.
802 Daza, J. D., E. L. Stanley, P. Wagner, A. M. Bauer, and D. A. Grimaldi. 2016. Mid-Cretaceous
803 amber fossils illuminate the past diversity of tropical lizards. Sci Adv 2:e1501080.
804 Eastman, J. M., M. E. Alfaro, P. Joyce, A. L. Hipp, and L. J. Harmon. 2011. A novel
805 comparative method for identifying shifts in the rate of character evolution on trees.
806 Evolution 65:3578-3589.
807 Eastman, J. M., D. Wegmann, C. Leuenberger, and L. J. Harmon. 2013. Simpsonian 'Evolution
808 by Jumps' in an adaptive radiation of *Anolis* lizards. arXiv preprint arXiv:1305.4216.
809 Emerson, S. B. 1991. The Ecomorphology of Bornean Tree Frogs (Family Rhacophoridae). Zool
810 J Linn Soc-Lond 101:337-357.
811 FitzJohn, R. G. 2012. Diversitree: comparative phylogenetic analyses of diversification in R.
812 Methods Ecol Evol 3:1084-1092.
813 Gamble, T., E. Greenbaum, T. R. Jackman, A. P. Russell, and A. M. Bauer. 2012. Repeated
814 origin and loss of adhesive toepads in geckos. PLoS ONE 7:e39429.
815 Gamble, T., E. Greenbaum, T. R. Jackman, A. P. Russell, and A. M. Bauer. 2017. Repeated
816 evolution of digital adhesion in geckos, a reply to Harrington and Reeder. J Evol Biol.
817 Garcia-Porta, J. and T. J. Ord. 2013. Key innovations and island colonization as engines of
818 evolutionary diversification: a comparative test with the Australasian diplodactyloid
819 geckos. J Evol Biol 26:2662-2680.
820 Haacke, W. 1976. The burrowing geckos of southern Africa, 5 (Reptilia: Gekkonidae). Annals of
821 the Transvaal Museum 30:71-89.
822 Hagey, T. J., J. B. Puthoff, K. E. Crandell, K. Autumn, and L. J. Harmon. 2016. Modeling
823 observed animal performance using the Weibull distribution. J Exp Biol 219:1603-1607.

824 Hagey, T. J., J. B. Puthoff, M. Holbrook, L. J. Harmon, and K. Autumn. 2014. Variation in setal
825 micromechanics and performance of two gecko species. Zoomorphology 133:111-126.
826 Hansen, T. F. 1997. Stabilizing selection and the comparative analysis of adaptation. Evolution
827 51:1341-1351.
828 Hansen, W. R. and K. Autumn. 2005. Evidence for self-cleaning in gecko setae. Proc. Natl.
829 Acad. Sci. USA 102:385-389.
830 Harmon, L. J., J. Baumes, C. Hughes, J. Soberon, C. D. Specht, W. Turner, C. Lisle, and R. W.
831 Thacker. 2013. Arbor: Comparative Analysis Workflows for the Tree of Life. PLoS
832 Currents 5:ecurrents.tol.099161de099165eabdee099073fd099163d099121a044518dc.
833 Harmon, L. J., J. A. Schulte, A. Larson, and J. B. Losos. 2003. Tempo and mode of evolutionary
834 radiation in iguanian lizards. Science 301:961-964.
835 Harmon, L. J., J. T. Weir, C. D. Brock, R. E. Glor, and W. Challenger. 2008. GEIGER:
836 investigating evolutionary radiations. Bioinformatics 24:129-131.
837 Harrington, S. and T. W. Reeder. 2017. Rate heterogeneity across Squamata, misleading
838 ancestral state reconstruction and the importance of proper null model specification. J
839 Evol Biol 30:313-325.
840 Higham, T. E., A. V. Birn-Jeffery, C. E. Collins, C. D. Hulsey, and A. P. Russell. 2015. Adaptive
841 simplification and the evolution of gecko locomotion: Morphological and biomechanical
842 consequences of losing adhesion. Proc Natl Acad Sci U S A 112:809-814.
843 Higham, T. E., T. Gamble, and A. P. Russell. 2016. On the origin of frictional adhesion in
844 geckos: small morphological changes lead to a major biomechanical transition in the
845 genus Gonatodes. Biol J Linn Soc.
846 Hu, S. H., S. Lopez, P. H. Niewiarowski, and Z. H. Xia. 2012. Dynamic self-cleaning in gecko
847 setae via digital hyperextension. J R Soc Interface 9:2781-2790.
848 Huber, G., S. N. Gorb, N. Hosoda, R. Spolenak, and E. Arzt. 2007. Influence of surface
849 roughness on gecko adhesion. Acta Biomater. 3:607-610.
850 Ingram, T. and D. L. Mahler. 2013. SURFACE: detecting convergent evolution from
851 comparative data by fitting Ornstein-Uhlenbeck models with stepwise Akaike
852 Information Criterion. Methods Ecol Evol 4:416-425.

Irish, F. J., E. E. Williams, and E. Seling. 1988. Scanning electron microscopy of changes in epidermal structure occurring during the shedding cycle in squamate reptiles. J Morphol 197:105-126.

Irschick, D. J., C. C. Austin, K. Petren, R. N. Fisher, J. B. Losos, and O. Ellers. 1996. A comparative analysis of clinging ability among pad-bearing lizards. Biol. J. Linn. Soc. 59:21-35.

Irschick, D. J., A. Herrel, and B. Vanhooydonck. 2006. Whole-organism studies of adhesion in pad-bearing lizards: creative evolutionary solutions to functional problems. J. Comp. Physiol. A 192:1169-1177.

Irschick, D. J., L. J. Vitt, P. A. Zani, and J. B. Losos. 1997. A comparison of evolutionary radiations in mainland and Caribbean Anolis lizards. Ecology 78:2191-2203.

Johnson, M. K. and A. P. Russell. 2009. Configuration of the setal fields of *Rhoptropus* (Gekkota: Gekkonidae): functional, evolutionary, ecological and phylogenetic implications of observed pattern. J Anat 214:937-955.

Lande, R. 1976. Natural-selection and random genetic drift in phenotypic evolution. Evolution 30:314-334.

Losos, J. B. 2009. Lizards in an evolutionary tree : the ecology of adaptive radiation in anoles. University of California Press, Berkeley.

Macrini, T. E., D. J. Irschick, and J. B. Losos. 2003. Ecomorphological differences in toepad characteristics between mainland and island anoles. J Herpetol 37:52-58.

Maddison, W. P. 2006. Confounding asymmetries in evolutionary diversification and character change. Evolution 60:1743-1746.

Maddison, W. P. and R. G. FitzJohn. 2015. The unsolved challenge to phylogenetic correlation tests for categorical characters. Syst Biol 64:127-136.

Maddison, W. P., P. E. Midford, and S. P. Otto. 2007. Estimating a binary character's effect on speciation and extinction. Syst Biol 56:701-710.

Maderson, P. 1970. Lizard hands and lizard glands: models for evolutionary study. Forma et Functio 3:179-204.

Maderson, P. F. A. 1964. Keratinized epidermal derivatives as an aid to climbing in gekkonid lizards. Nature 203:780-781.

McCool, J. I. 2012. Using the Weibull distribution: Reliability, modeling and inference. Wiley, Hoboken, NJ.

Mitchell, J. S. 2015. Extant-only comparative methods fail to recover the disparity preserved in the bird fossil record. Evolution 69:2414-2424.

Moen, D. S., D. J. Irschick, and J. J. Wiens. 2013. Evolutionary conservatism and convergence both lead to striking similarity in ecology, morphology and performance across continents in frogs. P R Soc B 280.

Nicholson, K. E., A. Mijares-Urrutia, and A. Larson. 2006. Molecular phylogenetics of the *Anolis onca* series: a case history in retrograde evolution revisited. J Exp Zool B Mol Dev Evol 306:450-459.

Oliver, P. M., A. M. Bauer, E. Greenbaum, T. Jackman, and T. Hobbie. 2012. Molecular phylogenetics of the arboreal Australian gecko genus *Oedura* Gray 1842 (Gekkota: Diplodactylidae): another plesiomorphic grade? Mol Phylogenet Evol 63:255-264.

Oliver, P. M. and P. Doughty. 2016. Systematic revision of the marbled velvet geckos (Oedura marmorata species complex, Diplodactylidae) from the Australian arid and semi-arid zones. Zootaxa 4088:151-176.

Peattie, A. M. 2007. The Function and Evolution of Gekkotan Adhesive Feet. Pp. 61. University of California, Berkeley, PhD Dissertation.

Peattie, A. M. 2008. Subdigital setae of narrow-toed geckos, including a eublepharid (*Aeluroscalabotes felinus*). Anat Rec 291:869-875.

Pennell, M. W., J. M. Eastman, G. J. Slater, J. W. Brown, J. C. Uyeda, R. G. FitzJohn, M. E. Alfaro, and L. J. Harmon. 2014. geiger v2.0: an expanded suite of methods for fitting macroevolutionary models to phylogenetic trees. Bioinformatics 30:2216-2218.

Persson, B. N. J. 2007. Biological adhesion for locomotion: basic principles. J. Adhesion Sci. Technol. 21:1145-1173.

Peterson, J. A. 1983. The evolution of the subdigital pad in Anolis. I. Comparisons among the anoline genera. Advances in herpetology and evolutionary biology: essays in honor of Ernest E. Williams:245-283.

Peterson, J. A. 1984. The microstructure of the scale surface in iguanid lizards. J Herpetol:437-467.

913 Peterson, J. A. and E. E. Williams. 1981. A case history in retrograde evolution: the *Onca*
914 lineage in anoline lizards. II. Subdigital fine structure. Bull. Mus. Comp. Zool. 149:215-
915 268.
916 Pianka, E. R. and S. L. Sweet. 2005. Integrative biology of sticky feet in geckos. BioEssays
917 27:647-652.
918 Pugno, N. M. and E. Lepore. 2008a. Living Tokay geckos display adhesion times following
919 Weibull Statistics. J. Adhesion 84:949-962.
920 Pugno, N. M. and E. Lepore. 2008b. Observation of optimal gecko's adhesion on nanorough
921 surfaces. BioSystems 94:218-222.
922 Pyron, R. A. and F. T. Burbrink. 2013. Early origin of viviparity and multiple reversions to
923 oviparity in squamate reptiles. Ecol Lett 17:13-21.
924 Rabosky, D. L. and E. E. Goldberg. 2015. Model inadequacy and mistaken inferences of trait-
925 dependent speciation. Syst Biol 64:340-355.
926 Rabosky, D. L. and E. E. Goldberg. 2017. FiSSE: A simple nonparametric test for the effects of a
927 binary character on lineage diversification rates. Evolution.
928 Revell, L. J. 2012. phytools: an R package for phylogenetic comparative biology (and other
929 things). Methods Ecol Evol 3:217-223.
930 Ruibal, R. 1968. The ultrastructure of the surface of lizard scales. Copeia 1968:698-703.
931 Ruibal, R. and V. Ernst. 1965. The structure of the digital setae of lizards. J. Morphol. 117:271-
932 293.
933 Russell, A. P. 1976. Some comments concerning interrelationships among gekkonine geckos. Pp.
934 217–244 *in* A. d. A. B. a. C. B. Cox, ed. Morphology and Biology of the Reptiles.
935 Linnean Society Symposium Series Number 3. Academic Press, London.
936 Russell, A. P. 1979. Parallelism and integrated design in the foot structure of gekkonine and
937 diplodactyline geckos. Copeia 1979:1-21.
938 Russell, A. P. 2002. Integrative Functional Morphology of the Gekkotan Adhesive System
939 (Reptilia: Gekkota). Integr. Comp. Biol. 42:1154-1163.
940 Russell, A. P., J. Baskerville, T. Gamble, and T. E. Higham. 2015. The evolution of digit form in
941 *Gonatodes* (Gekkota: Sphaerodactylidae) and its bearing on the transition from frictional
942 to adhesive contact in gekkotans. J Morphol 276:1311-1332.

943 Russell, A. P. and A. M. Bauer. 1988. Paraphalangeal elements of gekkonid lizards: a
944 comparative survey. J Morphol 197:221-240.
945 Russell, A. P. and M. K. Johnson. 2007. Real-world challenges to, and capabilities of, the
946 gekkotan adhesive system: contrasting the rough and the smooth. Can. J. Zool. 85:1228-
947 1238.
948 Russell, A. P. and M. K. Johnson. 2014. Between a rock and a soft place: microtopography of the
949 locomotor substrate and the morphology of the setal fields of Namibian day geckos
950 (Gekkota: Gekkonidae: *Rhoptropus*). Acta Zool 95:299-318.
951 Sadlier, R. A., D. O'Meally, and G. M. Shea. 2005. A new species of spiny-tailed gecko
952 (Squamata: Diplodactylidae: *Strophurus*) from Inland Queensland. Mem. Queensl. Mus.
953 51:573-582.
954 Sherratt, E., M. del Rosario Castañeda, R. J. Garwood, D. L. Mahler, T. J. Sanger, A. Herrel, K.
955 de Queiroz, and J. B. Losos. 2015. Amber fossils demonstrate deep-time stability of
956 Caribbean lizard communities. Proc. Natl. Acad. Sci. 112:9961-9966.
957 Stark, A. Y., T. W. Sullivan, and P. H. Niewiarowski. 2012. The effect of surface water and
958 wetting on gecko adhesion. J Exp Biol 215:3080-3086.
959 Stewart, G. R. and R. S. Daniel. 1972. Scales of Lizard Gekko-Gecko - Surface-Structure
960 Examined with Scanning Electron-Microscope. Copeia:252-&.
961 Stewart, G. R. and R. S. Daniel. 1975. Microornamentation of lizard scales: some variations and
962 taxonomic correlations. Herpetologica 31:117-130.
963 Tian, Y., N. Pesika, H. Zeng, K. Rosenberg, B. Zhao, P. McGuiggan, K. Autmn, and J.
964 Israelachvili. 2006. Adhesion and friction in gecko toe attachment and detachment. Proc.
965 Natl. Acad. Sci. USA 103:19320-19325.
966 Title, P. O. and D. L. Rabosky. 2016. Do Macrophylogenies Yield Stable Macroevolutionary
967 Inferences? An Example from Squamate Reptiles. Syst Biol.
968 Underwood, G. 1954. On the classification and evolution of geckos. Proc Zool Soc Lond
969 124:469-492.
970 Uyeda, J. C. and L. J. Harmon. 2014. A novel Bayesian method for inferring and interpreting the
971 dynamics of adaptive landscapes from phylogenetic comparative data. Syst Biol 63:902-
972 918.

973 Vanhooydonck, B., A. Andronescu, A. Herrel, and D. J. Irschick. 2005. Effects of substrate
974 structure on speed and acceleration capacity in climbing geckos. Biol J Linn Soc 85:385-
975 393.
976 Vucko, M. J. 2008. The dynamics of water on the skin of Australian carphodactyline and
977 diplodactyline geckos. Pp. 166. School of Marine and Tropical Biology. James Cook
978 University, Townsville, Queensland, Australia, Masters Thesis.
979 Wainwright, P. C. and S. M. Reilly. 1994. Ecological Morphology. University of Chicago Press,
980 Chicago IL.
981 Williams, E. E. and J. A. Peterson. 1982. Convergent and alternative designs in the digital
982 adhesive pads of scincid lizards. Science 215:1509-1511.
983 Wilson, S. and G. Swan. 2010. Complete Guide to Reptiles of Australia, 3rd ed. New Holland
984 Publishers, Chatswood, N.S.W.
985 Yoder, J. B., E. Clancey, S. Des Roches, J. M. Eastman, L. Gentry, W. Godsoe, T. J. Hagey, D.
986 Jochimsen, B. P. Oswald, J. Robertson, B. A. J. Sarver, J. J. Schenk, S. F. Spear, and L. J.
987 Harmon. 2010. Ecological opportunity and the origin of adaptive radiations. J Evol Biol
988 23:1581-1596.
989 Zenil-Ferguson, R. and M. W. Pennell. 2017. Digest: Trait-dependent diversification and its
990 alternatives. Evolution:n/a-n/a.
991